Title	GABA/glycine signaling during degeneration and regeneration of mouse hypoglossal nerves
Author(s)	Tatetsu, Masaharu; Kim, Jeongtae; Kina, Shinichiro; Sunakawa, Hajime; Takayama, Chitoshi
Citation	Brain Research, 1446: 22-33
Issue Date	2012-03-29
URL	http://hdl.handle.net/20.500.12000/46546
Rights	Creative Commons Attribution-NonCommercial-NoDerivatives 4.0

GABA/glycine signaling during degeneration and regeneration of mouse hypoglossal nerves

Masaharu Tatetsu[a,b], Jeongtae Kim[a], Shinichiro Kina[b], Hajime Sunakawa[b], and Chitoshi Takayama[a]*

[a]*Department of Molecular Anatomy, School of Medicine, University of the Ryukyus, Uehara 207, Nishihara, Okinawa, 9030215, Japan*

[b]*Department of Oral and Maxillofacial Functional Rehabilitation, School of Medicine, University of the Ryukyus, Uehara 207, Nishihara, Okinawa, 9030215, Japan*

* Corresponding author

Sections: Development, Degeneration and Regeneration, and Aging

Corresponding Author: Chitoshi Takayama

Department of Molecular Anatomy, School of Medicine, University of the Ryukyus, Uehara 207, Nishihara, Okinawa, 9030215, Japan

Phone: +81-98-895-1103

Fax: +81-98-895-1401

E-mail: takachan@med.u-ryukyu.ac.jp (C. Takayama)

ABSTRACT

In the adult central nervous system (CNS), GABA and glycine (Gly) are predominant inhibitory neurotransmitters, negatively regulating glutamatergic transmission. In the immature CNS, on the other hand, they act as trophic factors, mediating morphogenesis. In the present study, to investigate their involvement in axonal regeneration, we morphologically examined changes in their signaling in mouse hypoglossal nuclei during degeneration and regeneration of hypoglossal nerves. We found that (1) expression and localization of presynaptic elements were not changed, (2) localization of gephyrin, which anchors GABA and Gly receptors, was spread on the surface of motor neuron cell bodies and dendrites, (3) KCC2-expression markedly decreased, (4) choline acetyltransferase, which mediates acetylcholine-synthesis, immediately disappeared from the motor neurons, and (5) the synaptic cleft of both excitatory and inhibitory synapses became irregularly wider, in the hypoglossal nuclei of the sutured side after the operation. These changes gradually normalized during regeneration. These results suggested that (1) GABA/Gly, released from the presynaptic axon terminals or varicosities, may be spilled over the original synaptic cleft, be diffused into the neighboring space, bind the spread receptors, and mediate the depolarization of membrane potential of motor neurons, and (2) synthesis of acetylcholine may be stopped in the motor neurons, during Wallerian degeneration. Furthermore, it was suggested that

GABA/Gly signaling in postsynaptic motor neurons went back to be immature, and may play an important role in axonal regeneration.

Key words: choline acetyl transferase (ChAT), glutamic acid decarboxylase (GAD), gephyrin, hypoglossal nucleus, potassium chloride co-transporter 2 (KCC2), vesicular GABA transporter (VGAT)

Abbreviations

ABC: avidin-biotin-complex
Ach: acetylcholine
CC: central canal
ChAT: choline acetyl transferase
Cl^-: chloride ion
$[Cl^-]_i$: intracellular chloride concentration
CNS: central nervous system
CTB: cholera toxin B subunit
EPSP: excitatory postsynaptic potential
GABA: γ-amino butyric acid
GC: growth cone
GAD: glutamic acid decarboxylase
Gly: glycine
IPSP: inhibitory postsynaptic potential
KCC2: potassium chloride co-transporter 2
NMJ: neuromuscular junction
VGAT: vesicular GABA transporter
XII: hypoglossal nucleus
X: dorsal nucleus of vagus

1. Introduction

In the adult central nervous system (CNS), γ-amino butyric acid (GABA) is a predominant neurotransmitter, and mediates the hyperpolarization of membrane potential, negatively regulating the glutamatergic excitatory activity of neurons (Macdonald and Olsen, 1994; Olsen and Tobin, 1990). During brain development, on the other hand, GABA is an excitatory transmitter, serves as a trophic factor, and may be involved in controlling morphogenesis, such as regulating cell proliferation, cell migration, axonal growth, synapse formation, steroid- mediated sexual differentiation and cell death (Akerman and Cline, 2007; Andang et al., 2008; Ben-Ari, 2002; Ben-Ari et al., 2007; McCarthy et al., 2002; Owens and Kriegstein, 2002; Represa and Ben-Ari, 2005).

To reveal the morphological basis underlying the expression of GABAergic roles in brain development, we have investigated the developmental changes in GABA signaling in the cerebral cortex and cerebellum (Takayama and Inoue, 2004a; Takayama and Inoue, 2004b; Takayama, 2005; Takayama and Inoue, 2006; Takayama and Inoue, 2007; Takayama and Inoue, 2010). We found the common developmental “clockwise” changes. In the immature brain, GABA is localized throughout the axons, is extrasynaptically released, and binds immature type-GABA receptors, acts as an excitatory transmitter for several days before formation of GABAergic synapses. Subsequently, GABA and GABAergic vesicles are

confined to the axon varicosities and terminals, GABA receptors also accumulated to the postsynaptic site, GABAergic synapses are formed, and the GABAergic role shifts from excitation to inhibition.

Next, we focused on the GABAergic role in neuronal regeneration in the adult animal. We also focused on glycine (Gly) signaling, since Gly is a predominant inhibitory transmitter in the mature brain stem and spinal cord, and may act in the same manner as GABA signaling (Kirsch, 2006). It is commonly known that axons in the peripheral nervous system (PNS) successfully undergo regeneration, whereas those in the CNS could not, for about one century from Cajal (Cajal, 1928). Nevertheless, leading study by Aguayo (David and Aguayo, 1981) and many recent experiments (Benowitz and Popovich, 2010; Das et al., 2011; Okano, 2010; Renault-Mihara et al., 2008) indicated that neurons in the CNS as well as the PNS have the ability to re-extend their axons. The difference in success in PNS or failure in the CNS is considered to depend on the environment around the injured site of axons, indicating that the initial mechanism for axonal re-extension may be common in both the PNS and CNS. Taken together, we used the classical system of hypoglossal nerve cutting and suturing (Watson, 1968), to reveal the involvement of GABA and Gly in axonal regeneration.

To detect alteration in presynapse, postsynapse, and motor neurons during degeneration and regeneration, we examined the time-course of changes in expression and

localization of various molecules involved in GABA/Gly signaling and motor neuron functions after the hypoglossal nerve-operation. Choline acetyl transferase (ChAT), which mediates acetylcholine-synthesis, was a marker for the motor neuron activity. Synaptophysin, which is involved in vesicular release, was a marker for total presynaptic terminals. The vesicular GABA transporter (VGAT), which transports both GABA and Gly into synaptic vesicles, was a marker for inhibitory terminals. Glutamic acid decarboxylase (GAD), which is a synthetic enzyme of GABA (Barker et al., 1998; Martin and Rimvall, 1993), was a marker for GABA neurons, including GABAergic terminals. Gephyrin, which is an anchoring protein of both Gly receptors and GABA receptors (Fritschy et al., 2008; Kneussel and Betz, 2000; Tretter et al., 2008; Yu et al., 2007), was a marker of inhibitory transmitter receptors. Potassium sodium chloride co-transporter 2 (KCC2), which reduces intracellular chloride ion concentrations and shifts GABA action from excitation to inhibition (Ben-Ari, 2002; Owens and Kriegstein, 2002; Payne et al., 2003), was a marker for GABAergic inhibition. Furthermore, we examined the morphological changes in shapes of synapses by electron microscopy.

In the present study, we found “counterclockwise” shifts in the postsynaptic motor neurons, such as micro-separation between pre- and post-synapses, spread localization of receptors, down regunation of KCC2, and stopping of acetylcholine synthesis after axotomy

and their recovery after regeneration.

2. Results

2.1. Time-course of degeneration and regeneration

To examine the time-course of degeneration and regeneration of motor neurons and their axons, we performed Nissl staining and immunohistochemistry for CTB and ChAT. After hypoglossal nerves were resected, large neurons markedly decreased in number on Day 14, all large motor neurons disappeared on Day 21 (Fig.1A-E), and no CTB-labeling was detected in the operated side, although CTB continued to be localized within the cell bodies and proximal dendrites of large motor neurons (data not shown). After axons were sutured, on the other hand, no significant differences in the number and shape of large motor neurons were detected between sutured and intact sides (Fig.1F-J). CTB- immunolabeling was also not detected until Day 7 (Fig.1K, L). Several large neurons were labeled on Day 14 (arrows in Fig.1M), and the positive neurons markedly increased in number from Day 14 to Day 21 (Fig.1N, O). These results indicated that axons did not arrive at the tongue when 3-5mm axons were resected. The mouse hypoglossal neurons could not survive when axons were not renervated, as demonstrated in previous study (Kiryu-Seo et al., 2005). When axons were sutured, fastest axons arrived at tongue around Day 14, and majority of the axons renervated until Day 21, indicating that Wallerian degeneration immediately started after axotomy, and

majority of re-extended axons arrived at tongue during third post-operation week.

Both dorsal nuclei of vagus and intact hypoglossal nuclei continued to be occupied by ChAT-positive neurons after operation (Fig.1P-T). In contrast, large motor neurons did not express ChAT on Day 3 (Fig.1P). Only a few neurons expressed ChAT on Day 7 (arrows in Fig.1Q), and positive neurons markedly increased in number from Day 7 to Day 14 (Fig.1R). The majority of large neurons expressed ChAT, and the immunolabeling intensity of the sutured side became equal to that of the intact side after Day 21 (Fig.1S, T).

These results indicated that (1) neurons immediately stopped the synthesis of acetylcholine after cutting their axons, (2) re-extending hypoglossal axons first arrived at the tongue around Day 14, and the numbers of renervated axons markedly increased until Day 21, and (3) motor neurons started to synthesize acetylcholine several days before axon's arrival at the tongue.

2.2. Changes in immunohistochemical localization of synaptophysin, VGAT, and GAD in the hypoglossal nuclei after operation

To examine the changes in expression and localization of presynatpic elements, we performed imunohistochemistry for three molecules in the presynapse. We could not detect any changes in their expression of the sutured sides during degeneration and regeneration, or obvious differences in immunolabeling-intensity between intact and sutured sides (Fig.2-4). A

higher magnification views in both sides demonstrated that the immunolabeling of all molecules continued to exhibit fine dots during regeneration (Fig.2F-O, 3F-O, 4F-O). The dots were localized on the surface of cell bodies of motor neurons and neuropil region. We could not detect any apparent difference in the dot-density during degeneration and regeneration. Furthermore, we did not observe cell bodies, dendrites and axons filled by GAD-immunolabeling (Fig 4F-J) as detected in the developing cerebral cortex (Takayama and Inoue, 2010), cerebellum (Takayama and Inoue, 2004d) and spinal cord (Phelps et al., 1999; Tran et al., 2003).

These results suggested that axonal injury did not affect the expression and localization of presynaptic elements.

2.3. Change in immunohistochemical localization of gephyrin and KCC2 in hypoglossal nuclei after operation

To examine the changes in expression and localization of postsynaptic elements during degeneration and regeneration, we performed immunohistochemistry for gephyrin, as a marker of GABA and Gly receptors, and KCC2 as a marker of GABAergic inhibition. In the intact side, gephyrin-immunolabeling exhibited very tiny dots on the surface of the cell bodies of motor neurons and the neuropil, and the immunohistochemical staining pattern was not changed during regeneration (Fig. 5A). In the sutured side, on the other hand, the

gephyrin-immunolabeling became diffuse and dense on the cell membrane (asterisks) and dendrites (arrows) from Day 3 to Day 14 (Fig. 5B-D). Immunolabeling was gradually accumulated and exhibited fine dots on the cell bodies on Day 21 and Day 28 (Fig. 5E, F), but a little immunolabeling was still spread on Day 28 (Fig. 5F). This result suggested that GABA and Gly receptors were spread on the cell bodies and dendrites during degeneration and gradually re-accumulated during degeneration. Furthermore, since tiny dots continued to be detected in the neuropil region, GABA/Gly receptors on the interneurons may continue to accumulate in the postsynaptic sites (Fig. 5B-F).

KCC2-immunolabeling temporally reduced in intensity of the sutured side during degeneration and regeneration (Fig. 6A-C). The intensity of the sutured side was obviously lower than that in the intact side on Day 7 (Fig. 6B) and Day 14 (Fig. 6C). Immunolabeling gradually increased again after Day 14 (Fig. 6C-E). A higher magnification views in both sides demonstrated that KCC2 was not localized within the perikarya and nuclei but on the cell membrane of the dendrites and cell bodies during degeneration and regeneration (Fig. 6F-0). However, immunolabeling in the sutured side (Fig. 6G, H) was obviously weaker in compare to that of the intact side on Day 7 (Fig. 6L) and Day 14(Fig. 6M), in particular on the dendrites in the neuropil region. After Day 14, the immunolabeling in the neuropil gradually increased in the sutured side, (Fig. 6I, J)

2.4. A quantitative analysis of changes in expression of VGAT and KCC2 in hypoglossal nuclei after operation

In Figure2, we could not find any difference in immunolabeling-intensity of presynaptic elements between operated and intact sides on all post-operation days. In Figure 6, KCC2-expression reduced until Day 14, and increased again after that in the sutured side. To objectively examine the difference, we quantitatively measured the expression of VGAT, which is one of the presynaptic elements, and KCC2, which shift the GABA/Gly action from excitation to inhibition in the postsynapse, and examined the intensity ratio (operated side / intact side) by the Aperio® system. The VGAT-immunolabeling ratio (sutured side/intact side) did not change during degeneration and regeneration (Fig. 7A). In contrast, the KCC2-immunolabeling ratio was decreased to 77% on Day 3, 30% on Day 7, and 32% on Day 14 (Fig. 7B). After that it gradually increased to 60% on Day 21 and 66% on Day 28. Although we could not detect apparent difference in intensity, the ratio on Day 28 was significantly lower than that before the operation.

These results confirmed the results in Figure2-4 and 6, but KCC2-expression was not yet completely recovered to the normal level.

2.5 Electron microscopic changes in the hypoglossal nuclei of the sutred side

To examine the precise changes in the shapes of synapses after axotomy, we

performed electron microscopic analysis. We did not observe obvious degenerating axons and terminals. The shapes of presynapse, which contained spherical or flat vesicles and mitochondrion, were almost normal (Fig. 8A-C). Nevertheless, irregular large space was detected around the cell bodies of large motor neurons (Fig. 8A-C). The space completely (Fig. 8A) or partially (Fig. 8B, C) separated both inhibitory (right large terminal in Fig. 8C) and excitatory (other terminals in Fig. 8A-C) terminals from the motor neuron cell bodies. Process-like-structures sometimes invaded into the space (arrowheads in Fig. 8A, B). Postsynaptic density was observed at the intact area, where presynaptic- and postsynaptic membrane were closely faced (asterisks in Fig. 8 B, C), but was unclear at the separated regions, although high density areas were detected on the presynaptic membrane (asterisks in Fig. 8A). These changes were not detected in the intact side (data not shown).

These results indicated that the structure of presynapse was almost intact, but the synaptic cleft became irregularly wider and the post synaptic density was unclear at the separated regions.

3. Discussion

In the present study, we found obvious changes not in the presynapse but in the synaptic clefts and postsynaptic motor neurons during degeneration and regeneration. The

changes were schematically illustrated in the Figure 9.

3.1. Changes in presynase during degeneration

During Wallerian degeneration, expression and localization of three molecules, involved in synaptic transmission in the presynapse, did not change in the sutured side. The immunostaining of all these molecules exhibited tiny dots around and among large motor neurons. The density and intensity of the dots in the sutured side were equal to those in the intact side. In addition, we could not find any abnormalities in ultrastructure of presynapse. Previous studies reported that GABA and its synthetic enzyme, GAD, were diffusely distributed within the axons, cell bodies and dendrites during development of the cerebellum (Takayama and Inoue, 2010), cerebellum (Takayama and Inoue, 2004d) and spinal cord (Phelps et al., 1999; Tran et al., 2003). In the present study, however, we did not observe these patterns of GAD- and GABA- (data not shown) immunohistochemistry. These results suggested that GABA/Gly-ergic transmission continued to be mature in the presynapse.

3.2 Micro-separation between pre- and post- synapses

By electron microscopic analysis, we observed the irregular large space between motor neurons and presynapse as reported previously (Blinzinger and Kreutzberg, 1968; Cull, 1974; Fernando, 1971; Sumner, 1975; Torvik and Skjorten, 1971a; Torvik and Skjorten, 1971b). Process-like structure sometimes invaded the synaptic cleft. The complete

separation-type (Fig. 8A), however, was few, and we often observed partial or slight separation-type as Figure 8A and 8B, micro-separation. These changes were detected in both excitatory synapses, whose presynapse was occupied by spherical vesicles and inhibitory synapses, whose presynapse contained flat vesicles. Thick and thin post synaptic density in excitatory and inhibitory synapses, respectively, was limitedly detected at the postsynaptic membrane, where both pre- and post-synaptic membrane were closely faced, but was unclear at the separated area. Taken together these results, the transmitters, including glutamate, GABA and Gly may be normally released from presynaptic terminals, but spilled over the intact synaptic cleft, and diffused into large space.

3.3. Changes in postsynapse during degeneration

In postsynaptic motor neurons three apparent changes were detected during early degeneration stage. Firstly, gephyrin, which co-localized with Gly and GABA receptors (Fritschy et al., 2008; Kneussel and Betz, 2000; Tretter et al., 2008; Yu et al., 2007), was spread on the surface of the cell bodies and dendrites. After Day 14, immunolabeling gradually re-accumulated. These changes in distribution of receptor protein were quite similar to that of acetylcholine receptors during denervation and renervation of motor nerves (Anderson et al., 1977; Brenner and Sakmann, 1983; Frank and Fischbach, 1979; Schuetze and Vicini, 1984; Schuetze and Role, 1987). As mentioned in the previous paragraph, we

observed the micro-separation of synaptic clefts and unclearness of post synaptic density. These results indicated that the presynapse were morphologically and functionally separated from the post synapse, suggesting that the micro-separation might induce the spread of GABA/Gly receptors.

Secondly, KCC2-expession markedly decreased in the operated side on Day 7 and Day14. In particular, KCC2-positive dendrites became sparse in the neuropil. This result supported the previous reports using an *in situ* hybridization study (Nabekura et al., 2002). In the motor neurons, the efflux of chloride ions may be decreased due to the down regulation of KCC2 after the operation (Rivera et al., 1999), and the reduction in intracellular chloride ion concentration may induce the shift of GABA/Gly action from inhibition to excitation, mediating the depolarization of membrane potential. Direct triggers for the down-regulation of KCC2-expression are still unclear, but several mechanisms are speculated; for example (1) axotomy induced the brain derived neurotrophic factor (BDNF)-expression and the BDNF depressed the KCC2 expression (Aguado et al., 2003; Rivera et al., 2004; Shulga et al., 2008), and (2) micro-separation of synaptic contact stopped the KCC2 expression and so on (Ludwig et al., 2003; Takayama and Inoue, 2006).

Thirdly, ChAT immediately disappeared from motor neurons after axotomy. Since ChAT is a synthetic enzyme of acetylcholine, acetylcholine synthesis may immediately shut

down, indicating that acetylcholine release may also be stopped.

These three phenomena, detected in the synaptic cleft and post synaptic neurons (Fig. 7), were quite similar to these observed in the immature developing neurons, suggesting that axotomy induced a counterclockwise shift in GABA/Gly signaling from mature to immature stages (Takayama and Inoue, 2004c; Takayama, 2005).

3.4. Changes in GABA action during regeneration

The changes detected in postsynaptic motor neurons gradually normalized during regeneration. ChAT expression first recovered in the motor neurons from Day 7 to Day 14. The synthesis of acetylcholine re-started several days before axons arrived at the tongue, suggesting that acetylcholine may be extrasynaptically released from the axon terminals and could be involved in formation of the neuromuscular junction, including acetylcholine receptor accumulation. KCC2 gradually increased in expression after Day 14, indicating that GABA/Gly action was shifted from excitation to inhibition. The onset of the KCC2-increasing was concomitant to the massive axonal arrival at the target, tongue, suggesting that one of the cues for GABA/Gly action-shift may be the axonal renervation.

Furthermore, a quantitive analysis demonstrated that KCC2-intensity in the operated side was still significantly lower than that of the intact side, suggesting that a few neurons were still extending axons and receiving GABA/Gly as an excitatory transmitter.

Accumulation of gephyrin-immunolabeling and an increase in KCC2-expression occurred concomitantly after Day14. Since a little spread immunolabeling was detected on Day 28, micro-separation may remain and synapse re-formation may be still progressing or few presynapses were not formed synapses again as demonstrated previously (Sumner, 1976; Sumner, 1971).

3.5. Changes in GABA signaling after resection of hypoglossal nerves

We also examined the changes, when axons were not regenerated. A death of a large number of motor neurons occurred from Day 7 to Day 14, and all motor neurons disappeared on Day 28, indicating that hypoglossal neurons in the mouse brain could not survive when axons had not arrived at tongue. In the rat brain, on the other hand, the majority of large neurons survived 2 months after the same operation (Data not shown) as reported in previous papers (Kiryu-Seo et al., 2005), indicating that there may be a different mechanism for the neuronal survival between mouse and rat. VGAT- and gephyrin- expression gradually decreased after Day 14 as demonstrated in the rat facial nucleus after facial nerve axotomy (Eleore et al., 2004). Present result suggested that presynaptic elements gradually decreased in expression in the resected side after Day 14 due to the loss of target neurons. Motor neurons never expressed ChAT and KCC2 continued to decrease in expression after resection (Data not shown), suggesting that GABA may have intended to act as an excitatory transmitter after

axotomy, but could not survive.

4. Experimental Procedure

4.1. Animals and operation

We examined C57Bl/6J mice of postnatal day 30 to 40. Mice were deeply anesthetized by intra-peritoneal injection of a mixed solution (10μl/g body weight), containing 8% Nembutal® and 20% ethanol in saline. We performed two types of operation as shown in the Figure7. In one operation, after exposing left hypoglossal nerves (Fig. 8A), 3-5mm of hypoglossal nerves were resected between the digaster muscle and hyoid bone to prevent axonal regeneration to tongue (Fig. 8B, C). We did not find any connections between proximal and distal ends 28 days after the operation (data not shown). In the other operation, after cutting the axons just before dividing them into two major branches (bifurcation part) (arrowhead in Fig. 8A), both perineuriums of the proximal and distal nerve ends were immediately sutured with 10-0 Nylon (Fig. 8D, E).

4.2. Tracer injection

To examine the time-course of axonal renervation, cholera toxin B subunit (CTB, 5μg/mouse, List Biol Lab) was injected into the tongue under deep anesthesia, three days before fixation.

4.3. Antibodies

The list of primary antibodies used in the present study was shown in the Table 1.

4.4. Tissue preparation

Under deep anesthesia as above, mice were fixed by transcardial perfusion with fixative containing 4% paraformaldehyde in phosphate buffer (PB, 0.1M, pH 7.4) 3, 7, 14, 21, and 28 days after the operation (Day 3 etc.). Brains were removed from skulls, immersed in the same fixative overnight, and cryoprotected with 30% sucrose in PB for two days at 4°C. Brain stems were cut into coronal sections at a thickness of 20 ㎛ by a cryostat. The sections were mounted on gelatin-coated glass slides.

For the electron microscopic analysis, mice were fixed by mixed solution, containing 4% paraformaldehyde and 0.5% glutaraldehyde in PB on Day 7. Brain stems were cut into coronal sections at a thickness of 100㎛ by a microslicer. The sections were post-fixed by 1% OsO_4 in PB for 2 hours at 4°C, stained with 2% uranyl acetate aquarius solution overnight at room temperature, and embedded in epoxy resin in the usual manner. Ultra thin sections were stained with Sato's mixed lead solution (Sato, 1968) and observed under an electron microscope H-7500 (Hitachi, Japan).

4. 5 Immunohistochemistry for CTB, ChAT, synaptophysin, VGAT, GAD, gephyrin and

KCC2

Sections were treated as follows; with methanol containing 0.3% H_2O_2 for 30 min, PB for 10 min, 3% normal goat serum or normal rabbit serum in PB for 1h, and primary antibodies against CTB, ChAT, synaptophysin, VGAT, GAD, and KCC2 antibodies, overnight at room temperature. For gephyrin-immunohistochemistry, sections were treated with pepsin solution (1mg/ml) at 37°C for 10 min as described in a previous paper, followed by 3% normal goat serum for 1h and gephyrin antibody. After rinsing three times with PB for 15 min, sections were visualized by the avidin-biotin-peroxidase complex (ABC) method with Histofine kit (Nichirei, Japan).

4.6. Image analysis of the IHC

We analyzed the changes in immunolabeling intensity of VGAT (7-13 mice/each post-operation day, average number= 10.0) and KCC2 (9-28 mice/each post-operation day, average number= 17.3) in hypoglossal nuclei using Aperio Scanscpe（Positive Pixel Count Ver. 9）. After adjusting the background immunolabeling intensity to the ependymocytes around the central canal, we measured the immunostaining density of intact and sutured sides by Positive Pixel Count, and calculated the ratio between them during regeneration.

Statistical analysis was done by T-test.

These experiments were approved by the Animal Care and Use Committees of University of the Ryukyus (No. 4683, No.5205) and were performed in conformance with the *Guide for the Care and Use of Laboratory Animals of University of the Ryukyus*. Every effort was made to minimize the number of animals and their suffering.

Acknowledgements

We are grateful to Makiko Moriyasu-Kuroki and Yukiji Yabiku at the Department of Molecular Anatomy for their assistance in the preparation of this manuscript. We would also like thank Prof. Fuminori Kanaya at the Department of Orthopedics for his advice on the nerve operation technique, and Hidemichi Kin and Yoshinori Kosaka at the Department of Molecular Anatomy for the valuable discussion. This work was supported by the grants-in-aid from the Ministry of Education, Science, Sports and Culture of Japan (Kiban C No. 20500310, No. 23500413), Uruma Science Foundation, and Takeda Science Foundation.

Figure legends

Figure 1 Changes in cytoarchitecture (A-J), CTB labeling (K-O) and ChAT-immunohistochemistry (P-T), 3 (Day3, A, F, K), 7 (Day7, B, G, L), 14 (Day14, C, H, M), 21 (Day21, D, I, O), and 28 (Day28, E, J, P) days after the left hypoglossal nerves were resected (A-E) and sutured (F-T).

A-E: Hypoglossal nuclei (XII) and dorsal nuclei of vagus (X) stained by toluidine blue after axons were resected.

F-J: Toluidine blue staining after axons were sutured.

K-O: Hypoglossal neurons containing CTB, which was transported from the tongue. Several neurons (arrows) became positive in the sutured side on Day 14 (H).

P-T: Immunohistochemistry for ChAT. Several neurons (arrows) re-expressed the ChAT on Day 7 (L).

Scale bar: 50μm

Figure 2 Changes in immunochemical localization of synaptophysin on Day 3 (A, F, K), Day 7 (B, G, L), Day 14 (C, H, M), Day 21 (D, I, N), and Day 28 (E, J, O) in the brain stem at lower magnification (A-E) and in the hypoglossal nucleus of sutured side (F-J) and intact side (K-O) at higher magnification.

No apparent differences in immunolabeling-intensity and dot-density were detected

between sutured (left) and intact (right) side of hypoglossal nuclei throughout the degeneration and regeneration.

Abbreviations and symbols: CC: central channel, X: dorsal nucleus of vagus, XII: hypoglossal nucleus, asterisk: large motor neuron

Scale bar: 50μm

Figure 3 Changes in immunochemical localization of VGAT on Day 3 (A, F, K), Day 7 (B, G, L), Day 14 (C, H, M), Day 21 (D, I, N), and Day 28 (E, J, O) in the brain stem at lower magnification (A-E) and in the hypoglossal nucleus of sutured side (F-J) and intact side (K-O) at higher magnification.

No apparent differences in immunolabeling-intensity and dot-density were detected between sutured (left) and intact (right) side of hypoglossal nuclei throughout the degeneration and regeneration.

Abbreviations and symbols: CC: central channel, X: dorsal nucleus of vagus, XII: hypoglossal nucleus, asterisk: large motor neuron

Scale bar: 50μm

Figure 4 Changes in immunochemical localization of GAD on Day 3 (A, F, K), Day 7 (B, G, L), Day 14 (C, H, M), Day 21 (D, I, N), and Day 28 (E, J, O) in the brain stem at lower magnification (A-E) and in the hypoglossal nucleus of sutured side (F-J) and intact side (K-O)

at higher magnification.

No apparent differences in immunolabeling-intensity and dot-density were detected between sutured (left) and intact (right) side of hypoglossal nuclei throughout the degeneration and regeneration.

Abbreviations and symbols: CC: central channel, X: dorsal nucleus of vagus, XII: hypoglossal nucleus, asterisk: large motor neuron

Scale bar: 50μm

Figure 5 Immunohistochemistry for gephyrin at higher magnification

A: Gephyrin-immunohistochemistry of the intact side on Day 7.

Tiny dots were scattered in the neuropil region and attached on the surface of motor neuron cell bodies (asterisks).

B-F: Changes in gephyrin localization on Day 3 (B), Day 7 (C), Day 14 (D), Day 21 (E) and Day 28 (F). Dense immunolabeling (arrowheads) was spread on the surface of the cell bodies (asterisks) and dendrites from Day 3 to Day14 (B-D). The spread immunolabeling gradually decreased from Day 21 (D, E).

Scale bar: 20μm

Figure 6 Changes in immunohistochemical localization of KCC2 at lower- (A-E) and higher-magnification (F-O) of sutured (F-J) and intact (K-O) sides, 3 (Day3, A, F, K), 7 (Day7,

B, G, L), 14 (Day14, C, H, M), 21 (Day21, D, I, N), and 28 (Day28, E, J, O) days after the axons were sutured.

Abbreviations and symbols: CC: central channel, X: dorsal nucleus of vagus, XII: hypoglossal nucleus, asterisk: motor neuron cell body

Scale bar: 50μm

Figure 7 A quantitative analysis of changes in the immunolabeling-intensity of VGAT (A) and KCC2 (B)

No significant changes in VGAT-intensity were detected during degeneration and regeneration (A), whereas KCC2 markedly decreased in expression after operation.

***P<0.001,

Error bars indicate the standard error (SE).

Figure 8 Electron micrographs of the hypoglossal nucleus of sutured side on Day 7

A: Large space separated (arrows) two terminals (T) from the motor neuron cell (MN) body. Process-like-structure (arrowheads) was observed within the space. Although thin high density areas (asterisks) were detected on the presynaptic membrane, no high density area was detected on the counter part.

B: Two terminals (T), both of which may be excitatory, were formed synapses with motor neuron (MN) cell body (asterisks). Large space (arrows) and process-like-structure

(arrowheads) were detected between presynapse and postsynapse. High density (asterisk) area was detected on the postosynaptic membrane at the intact synaptic area.

C: Two terminals (T) were formed synapses with motor neuron (MN) cell bodies (asterisks). The right large terminal may be inhibitory, since flat vesicles were sparsely detected within the terminals, and the post synaptic density (asterisks) was thin and symmetrical. Large space (arrows) was irregularly detected between pre- and post synaptic membrane.

Scale bar: 1μm

Figure 9 Schematic illustrations of the changes in GABA/Gly signaling before axotomy (A) and during regeneration (B)

A: GABA/Gly signaling before axotomy

The motor neuron receives GABA/Gly-ergic input on the cell body. Synaptically released GABA/Gly binds to their receptor, mediating an inhibitory post synaptic potential (IPSP) by way of chloride ion (Cl^-) efflux , since KCC2 transports Cl^- out of the cell bodies. In the motor neuron, acethocholine (Ach) is synthesized with acetate (acetyl-CoA) and choline by ChAT and released at the neuromuscular junction (NMJ) on the skeletal muscle (tongue).

B: GABA/Gly signaling during degeneration

After axotomy, the axon is re-extending under the growth cone (GC) guidance along

basal lamina. GABA/Gly-ergic terminals slightly separate from the postsynaptic membrane (micro-separation), and the receptor protein were spread on the cell membrane. Released GABA/Gly is spilled over the synaptic site, binds to perisynaptic receptor, and induces the depolarization of membrane potential (excitatory postsynaptic potential EPSP), since KCC2-expression decreased and intracellular chloride condentration ([Cl-]i) become higher. ChAT-synthesis also is stopped and acetylcholine is not released from the neurons.

Figure 10 Operation procedure

A: The left hypoglossal nerve was exposed, and was cut at the arrowhead position.

B: Photograph showing the resected part of hypoglossal nerve (between arrowheads).

C: Schematic illustration shown in B.

D: Photograph showing the sutured nerve (arrowheads).

E: Schematic illustration shown in D.

Scale bar: 1mm

References

Aguado, F., Carmona, M.A., Pozas, E., Aguilo, A., Martinez-Guijarro, F.J., Alcantara, S., Borrell, V., Yuste, R., Ibanez, C.F., Soriano, E., 2003. BDNF regulates spontaneous correlated activity at early developmental stages by increasing synaptogenesis and expression of the K+/Cl- co-transporter KCC2. Development. 130**,** 1267-80.

Akerman, C.J., Cline, H.T., 2007. Refining the roles of GABAergic signaling during neural circuit formation. Trends Neurosci. 30**,** 382-9.

Andang, M., Hjerling-Leffler, J., Moliner, A., Lundgren, T.K., Castelo-Branco, G., Nanou, E., Pozas, E., Bryja, V., Halliez, S., Nishimaru, H., Wilbertz, J., Arenas, E., Koltzenburg, M., Charnay, P., El Manira, A., Ibanez, C.F., Ernfors, P., 2008. Histone H2AX-dependent GABA(A) receptor regulation of stem cell proliferation. Nature. 451**,** 460-4.

Anderson, M.J., Cohen, M.W., Zorychta, E., 1977. Effects of innervation on the distribution of acetylcholine receptors on cultured muscle cells. J Physiol. 268**,** 731-56.

Barker, J.L., Behar, T., Li, Y.X., Liu, Q.Y., Ma, W., Maric, D., Maric, I., Schaffner, A.E., Serafini, R., Smith, S.V., Somogyi, R., Vautrin, J.Y., Wen, X.L., Xian, H., 1998. GABAergic cells and signals in CNS development. Perspect Dev Neurobiol. 5**,** 305-22.

Ben-Ari, Y., 2002. Excitatory actions of gaba during development: the nature of the nurture. Nat Rev Neurosci. 3**,** 728-39.

Ben-Ari, Y., Gaiarsa, J.L., Tyzio, R., Khazipov, R., 2007. GABA: a pioneer transmitter that excites immature neurons and generates primitive oscillations. Physiol Rev. 87**,** 1215-84.

Benowitz, L.I., Popovich, P.G., 2010. Inflammation and axon regeneration. Curr Opin Neurol. 24**,** 577-83.

Blinzinger, K., Kreutzberg, G., 1968. Displacement of synaptic terminals from regenerating motoneurons by microglial cells. Z Zellforsch Mikrosk Anat. 85**,** 145-57.

Brenner, H.R., Sakmann, B., 1983. Neurotrophic control of channel properties at neuromuscular synapses of rat muscle. J Physiol. 337**,** 159-71.

Cajal, R.y., S, 1928. Degeneration and regeneration of the nervous system (Translated by RM Day from the 1913 Spanish edition). Vol., Oxford University Press, Oxford.

Cull, R.E., 1974. Role of nerve-muscle contact in maintaining synaptic connections. Exp Brain Res. 20**,** 307-10.

Das, A.K., Gopurappilly, R., Parhar, I., 2011. Current status and prospective application of stem cell-based therapies for spinal cord injury. Curr Stem Cell Res Ther. 6**,** 93-104.

David, S., Aguayo, A.J., 1981. Axonal elongation into peripheral nervous system "bridges" after central nervous system injury in adult rats. Science. 214**,** 931-3.

Eleore, L., Vassias, I., Vidal, P.P., de Waele, C., 2004. An in situ hybridization and immunofluorescence study of glycinergic receptors and gephyrin in the vestibular nuclei of the intact and unilaterally labyrinthectomized rat. Exp Brain Res. 154, 333-44.

Fernando, D.A., 1971. A third glial cell seen in retrograde degeneration of the hypoglossal nerve. Brain Res. 27, 365-8.

Frank, E., Fischbach, G.D., 1979. Early events in neuromuscular junction formation in vitro: induction of acetylcholine receptor clusters in the postsynaptic membrane and morphology of newly formed synapses. J Cell Biol. 83, 143-58.

Fritschy, J.M., Harvey, R.J., Schwarz, G., 2008. Gephyrin: where do we stand, where do we go? Trends Neurosci. 31, 257-64.

Kirsch, J., 2006. Glycinergic transmission. Cell Tissue Res. 326, 535-40.

Kiryu-Seo, S., Hirayama, T., Kato, R., Kiyama, H., 2005. Noxa is a critical mediator of p53-dependent motor neuron death after nerve injury in adult mouse. J Neurosci. 25, 1442-7.

Kneussel, M., Betz, H., 2000. Clustering of inhibitory neurotransmitter receptors at developing postsynaptic sites: the membrane activation model. Trends Neurosci. 23, 429-35.

Ludwig, A., Li, H., Saarma, M., Kaila, K., Rivera, C., 2003. Developmental up-regulation of KCC2 in the absence of GABAergic and glutamatergic transmission. Eur J Neurosci. 18, 3199-206.

Macdonald, R.L., Olsen, R.W., 1994. GABAA receptor channels. Annu Rev Neurosci. 17, 569-602.

Martin, D.L., Rimvall, K., 1993. Regulation of gamma-aminobutyric acid synthesis in the brain. J Neurochem. 60, 395-407.

McCarthy, M.M., Auger, A.P., Perrot-Sinal, T.S., 2002. Getting excited about GABA and sex differences in the brain. Trends Neurosci. 25, 307-12.

Nabekura, J., Ueno, T., Okabe, A., Furuta, A., Iwaki, T., Shimizu-Okabe, C., Fukuda, A., Akaike, N., 2002. Reduction of KCC2 expression and GABAA receptor-mediated excitation after in vivo axonal injury. J Neurosci. 22, 4412-7.

Okano, H., 2010. Neural stem cells and strategies for the regeneration of the central nervous system. Proc Jpn Acad Ser B Phys Biol Sci. 86, 438-50.

Olsen, R.W., Tobin, A.J., 1990. Molecular biology of GABAA receptors. Faseb J. 4, 1469-80.

Owens, D.F., Kriegstein, A.R., 2002. Is there more to GABA than synaptic inhibition? Nat Rev Neurosci. 3, 715-27.

Payne, J.A., Rivera, C., Voipio, J., Kaila, K., 2003. Cation-chloride co-transporters in neuronal communication, development and trauma. Trends Neurosci. 26, 199-206.

Phelps, P.E., Alijani, A., Tran, T.S., 1999. Ventrally located commissural neurons express the GABAergic phenotype in developing rat spinal cord. J Comp Neurol. 409**,** 285-98.

Renault-Mihara, F., Okada, S., Shibata, S., Nakamura, M., Toyama, Y., Okano, H., 2008. Spinal cord injury: emerging beneficial role of reactive astrocytes' migration. Int J Biochem Cell Biol. 40**,** 1649-53.

Represa, A., Ben-Ari, Y., 2005. Trophic actions of GABA on neuronal development. Trends Neurosci. 28**,** 278-83.

Rivera, C., Voipio, J., Payne, J.A., Ruusuvuori, E., Lahtinen, H., Lamsa, K., Pirvola, U., Saarma, M., Kaila, K., 1999. The K+/Cl- co-transporter KCC2 renders GABA hyperpolarizing during neuronal maturation. Nature. 397**,** 251-5.

Rivera, C., Voipio, J., Thomas-Crusells, J., Li, H., Emri, Z., Sipila, S., Payne, J.A., Minichiello, L., Saarma, M., Kaila, K., 2004. Mechanism of activity-dependent downregulation of the neuron-specific K-Cl cotransporter KCC2. J Neurosci. 24**,** 4683-91.

Sato, T., 1968. A modified method for lead staining of thin sections. J Electron Microsc (Tokyo). 17**,** 158-9.

Schuetze, S.M., Vicini, S., 1984. Neonatal denervation inhibits the normal postnatal decrease in endplate channel open time. J Neurosci. 4**,** 2297-302.

Schuetze, S.M., Role, L.W., 1987. Developmental regulation of nicotinic acetylcholine receptors. Annu Rev Neurosci. 10**,** 403-57.

Shulga, A., Thomas-Crusells, J., Sigl, T., Blaesse, A., Mestres, P., Meyer, M., Yan, Q., Kaila, K., Saarma, M., Rivera, C., Giehl, K.M., 2008. Posttraumatic GABA(A)-mediated [Ca2+]i increase is essential for the induction of brain-derived neurotrophic factor-dependent survival of mature central neurons. J Neurosci. 28**,** 6996-7005.

Sumner, 1976. Quantitative ultrastructural observations on the inhibited recovery of the hypoglossal nucleus from the axotomy response when regeneration of the hypoglossal nerve is prevented. Exp Brain Res. 26**,** 141-150.

Sumner, B., 1975. A quantitative analysis of the response of presynaptic boutons to postsynaptic motor neuron axotomy. Exp Neurol. 46**,** 605-615.

Sumner, W., 1971. Retraction and expansion of the dendritic tree of motor neurones of adult rats induced in vivo. Nature. 233**,** 273-275.

Takayama, C., Inoue, Y., 2004a. Transient expression of GABA(A) receptor alpha2 and alpha3 subunits in differentiating cerebellar neurons. Brain Res Dev Brain Res. 148**,** 169-77.

Takayama, C., Inoue, Y., 2004b. Extrasynaptic localization of GABA in the developing mouse cerebellum. Neurosci Res. 50**,** 447-58.

Takayama, C., Inoue, Y., 2004c. GABAergic signaling in the developing cerebellum. Anat Sci

Int. 79, 124-136.
Takayama, C., Inoue, Y., 2004d. Morphological development and maturation of the GABAergic synapses in the mouse cerebellar granular layer. Brain Res Dev Brain Res. 150, 177-90.
Takayama, C., 2005. GABAergic signaling in the developing cerebellum. Int Rev Neurobiol. 71, 63-94.
Takayama, C., Inoue, Y., 2006. Developmental localization of potassium chloride co-transporter 2 in granule cells of the early postnatal mouse cerebellum with special reference to the synapse formation. Neuroscience. 143, 757-67.
Takayama, C., Inoue, Y., 2007. Developmental localization of potassium chloride co-transporter 2 (KCC2) in the Purkinje cells of embryonic mouse cerebellum. Neurosci Res. 57, 322-5.
Takayama, C., Inoue, Y., 2010. Developmental localization of potassium chloride co-transporter 2 (KCC2), GABA and vesicular GABA transporter (VGAT) in the postnatal mouse somatosensory cortex. Neurosci Res. 67, 137-48.
Torvik, A., Skjorten, F., 1971a. Electron microscopic observations on nerve cell regeneration and degeneration after axon lesions. II. Changes in the glial cells. Acta Neuropathol. 17, 265-82.
Torvik, A., Skjorten, F., 1971b. Electron microscopic observations on nerve cell regeneration and degeneration after axon lesions. I. Changes in the nerve cell cytoplasm. Acta Neuropathol. 17, 248-64.
Tran, T.S., Alijani, A., Phelps, P.E., 2003. Unique developmental patterns of GABAergic neurons in rat spinal cord. J Comp Neurol. 456, 112-26.
Tretter, V., Jacob, T.C., Mukherjee, J., Fritschy, J.M., Pangalos, M.N., Moss, S.J., 2008. The clustering of GABA(A) receptor subtypes at inhibitory synapses is facilitated via the direct binding of receptor alpha 2 subunits to gephyrin. J Neurosci. 28, 1356-65.
Watson, W.E., 1968. Observations on the nucleolar and total cell body nucleic acid of injured nerve cells. J Physiol. 196, 655-76.
Yu, W., Jiang, M., Miralles, C.P., Li, R.W., Chen, G., de Blas, A.L., 2007. Gephyrin clustering is required for the stability of GABAergic synapses. Mol Cell Neurosci. 36, 484-500.

Table 1 Antibody characterization

Antigen	Immunogen	Manufacture Species, etc. Reference	Dilution used
Choline acetyransferase (ChAT)	Human placental enzyme	AB144, Chemicon, Millpore	Final concentration 1µg/ml
Chlera toxin B Subunt(CTB)	High titer polyclonal anti-choleragenoid from goat	List Biological Lab #703	Final concentration 0.1µg/ml
Gultamic acid decarboxylase (GAD)	A synthetic peptide wuth the amino acid sequence [C]DFLIEEIERLGQDL From rat	AB1511, Chemicon Millpore	Final concentration 1:2000
gephyrin	mouse monoclonal antibody raised against amino scids 437-736 of gephyrin of human origin	Santa Cruze, SC25311	Final concentration 1:60000
Potassium chloride Co-transporter 2 (KCC2)	Synthetic peptide, aa 44-64 from N-terminals of mouse	Original antibody, Rabbit, polyclonal, Takayama and Inoue(2006)	Final concentration 1µg/ml
synaptophysin	Rabbit anti-synaptophysin	Zymed No. 08-1130	Final concentration 1µg/ml
Vesicular GABA Trnceprter (VGAT)	Synthetic peptide, aa 1022-1042 from N-terminals of mouse	Original antibody, Rabbit, polyclonal, Takayama and Inoue(2004)	Final concentration 1µg/ml

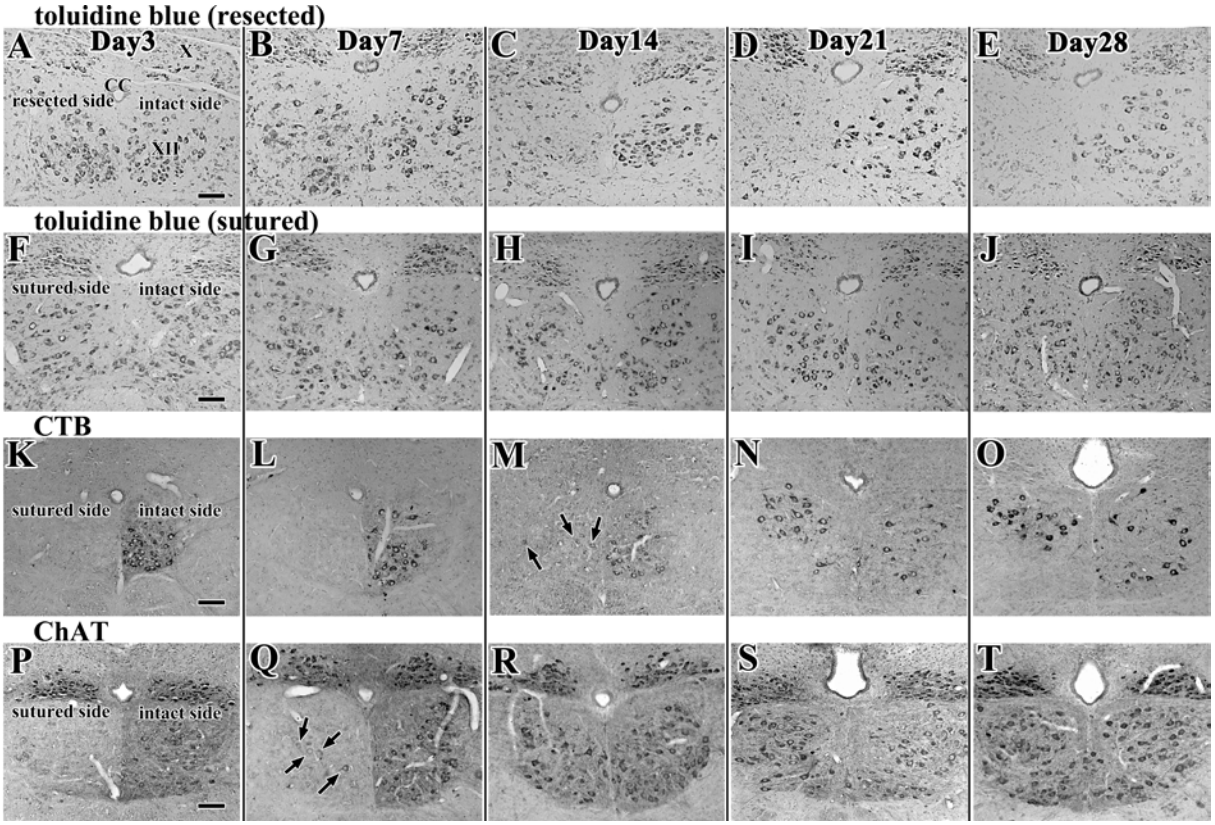
toluidine blue (resected)
A Day3
X
CC
resected side
intact side
XII
B Day7
C Day14
D Day21
E Day28
toluidine blue (sutured)
F
sutured side
intact side
G
H
I
J
CTB
K
sutured side
intact side
L
M
N
O
ChAT
P
sutured side
intact side
Q
R
S
T

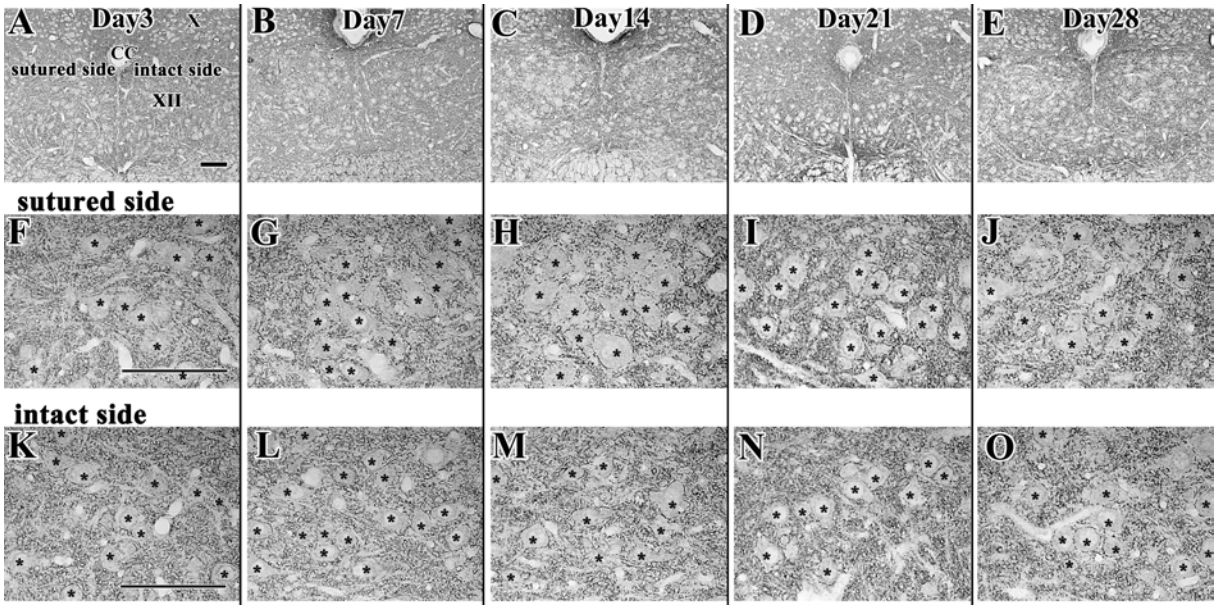
A Day3
X
CC
sutured side
intact side
XII
B Day7
C Day14
D Day21
E Day28
sutured side
F
G
H
I
J
intact side
K
L
M
N
O

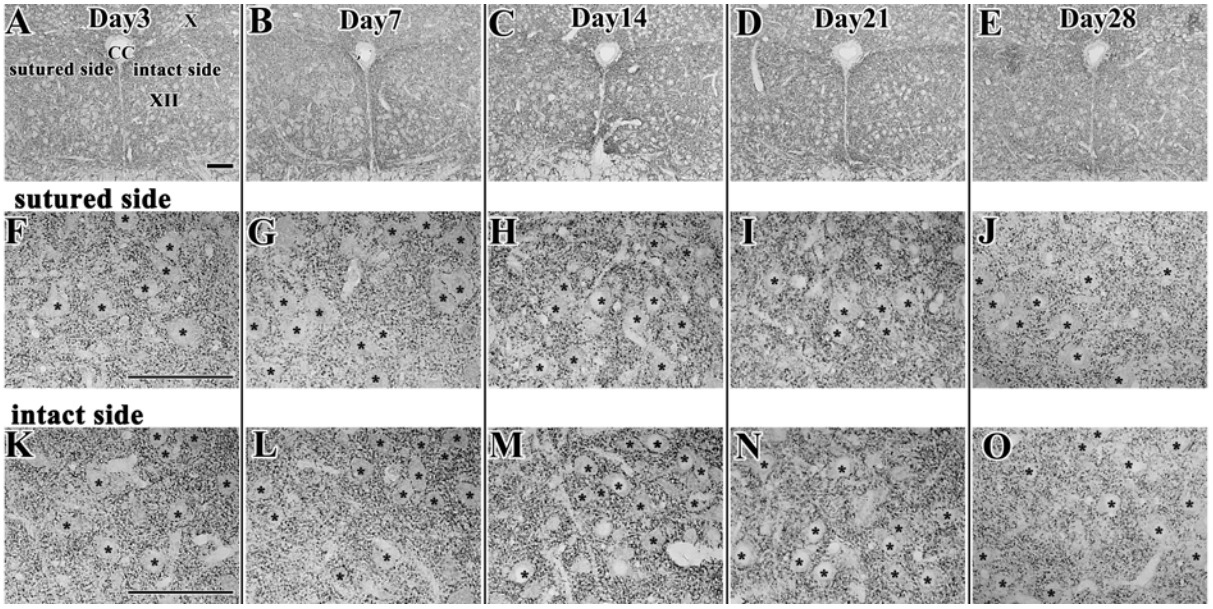
A
Day3
X
CC
sutured side
intact side
XII
B
Day7
C
Day14
D
Day21
E
Day28
sutured side
F
G
H
I
J
intact side
K
L
M
N
O

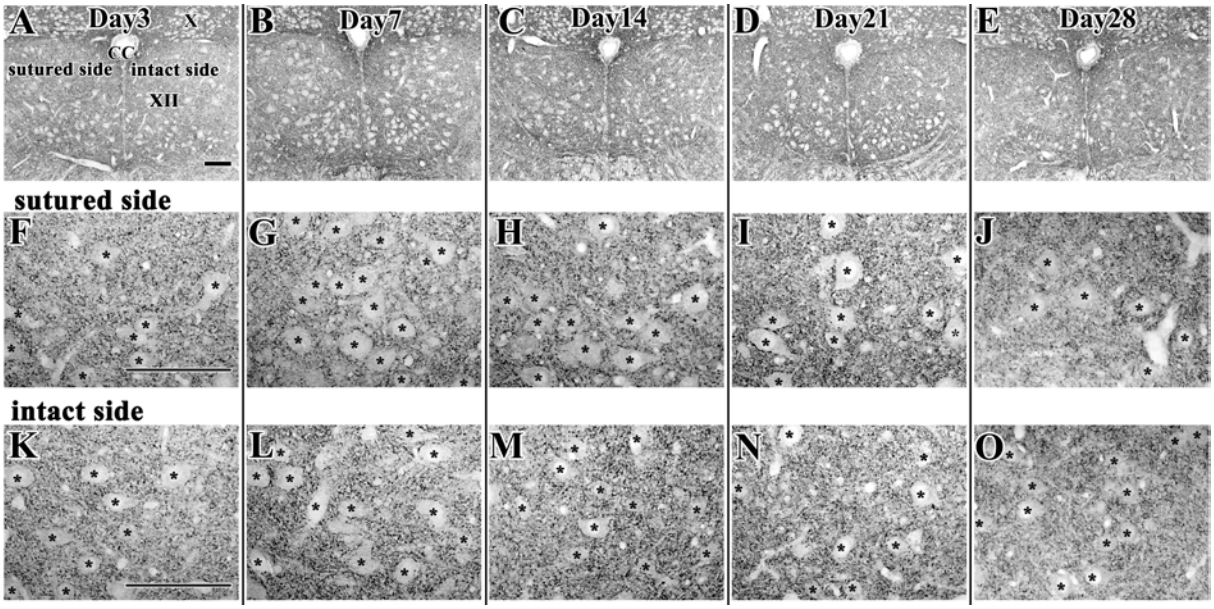
A
Day3
X
CC
sutured side
intact side
XII
B
Day7
C
Day14
D
Day21
E
Day28
sutured side
F
G
H
I
J
intact side
K
L
M
N
O

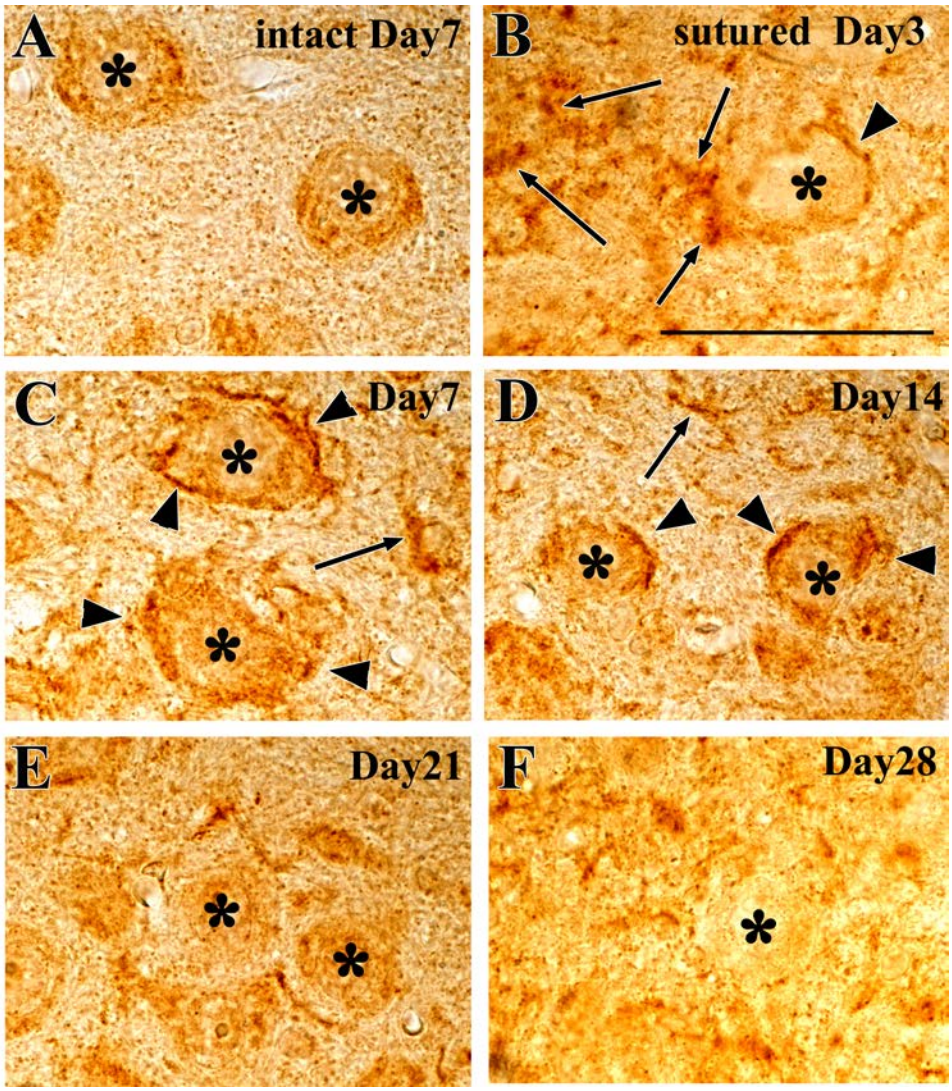
A
intact Day7
B
sutured Day3
C
Day7
D
Day14
E
Day21
F
Day28

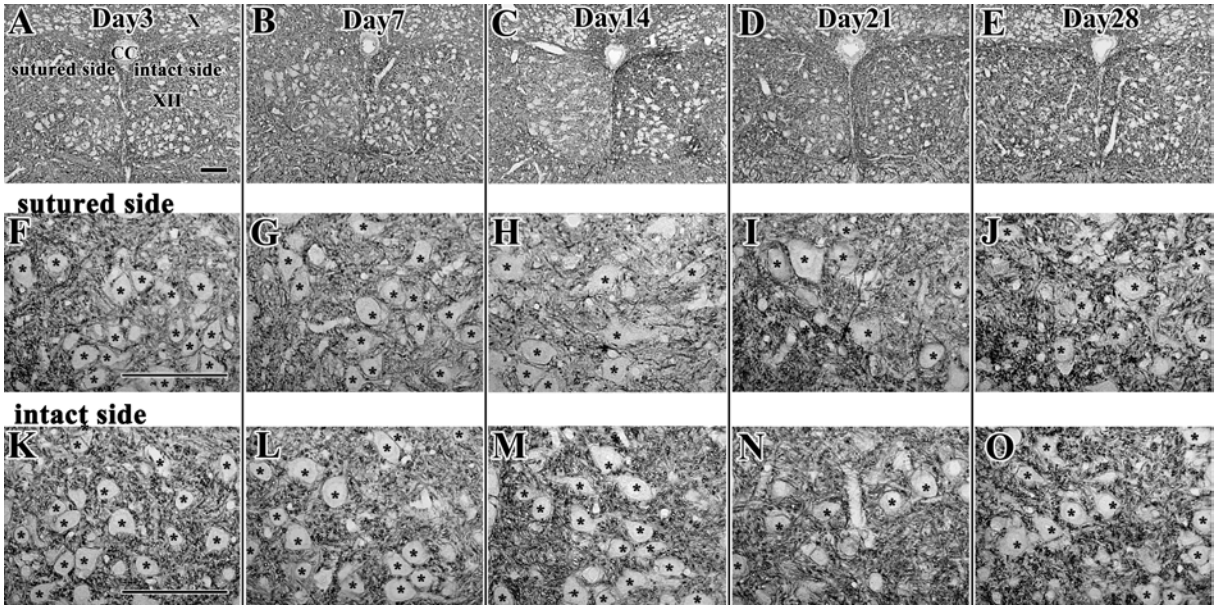
A
Day3
CC
sutured side
intact side
XII
B
Day7
C
Day14
D
Day21
E
Day28
sutured side
F
G
H
I
J
intact side
K
L
M
N
O

A

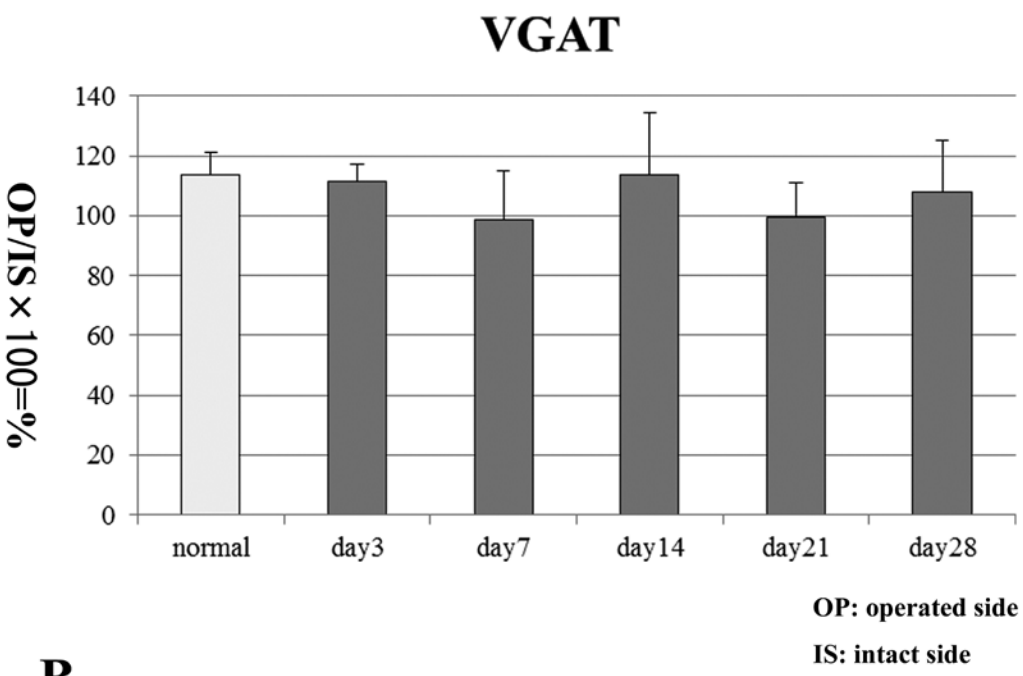
VGAT
OP/IS × 100=%
140
120
100
80
60
40
20
0
normal
day3
day7
day14
day21
day28
OP: operated side
IS: intact side

B

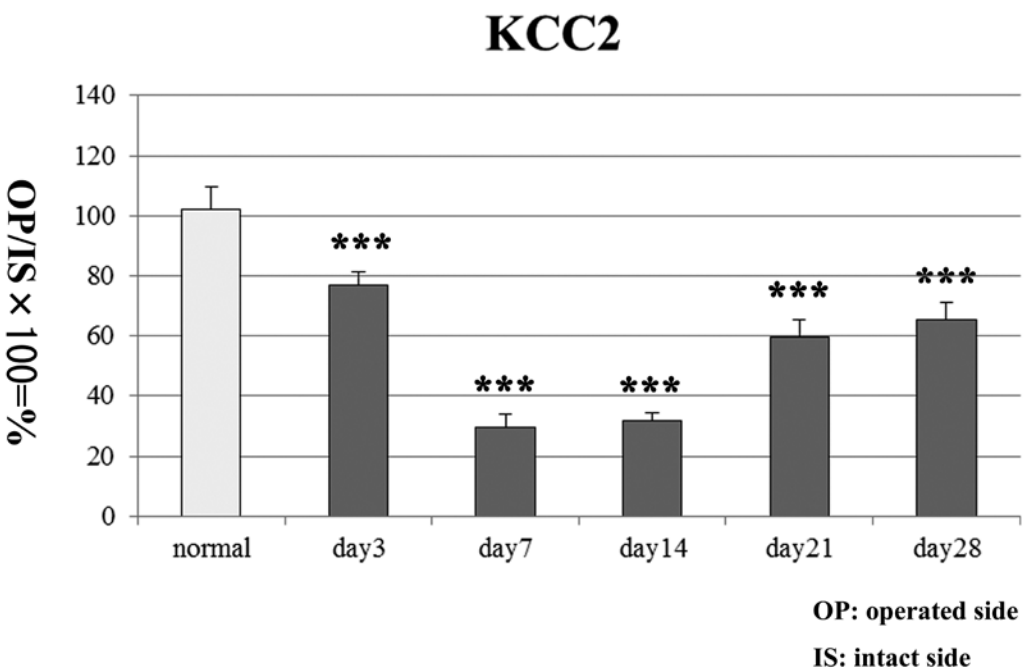
KCC2
OP/IS × 100=%
140
120
100
80
60
40
20
0
***
***
***
***
***
normal
day3
day7
day14
day21
day28
OP: operated side
IS: intact side

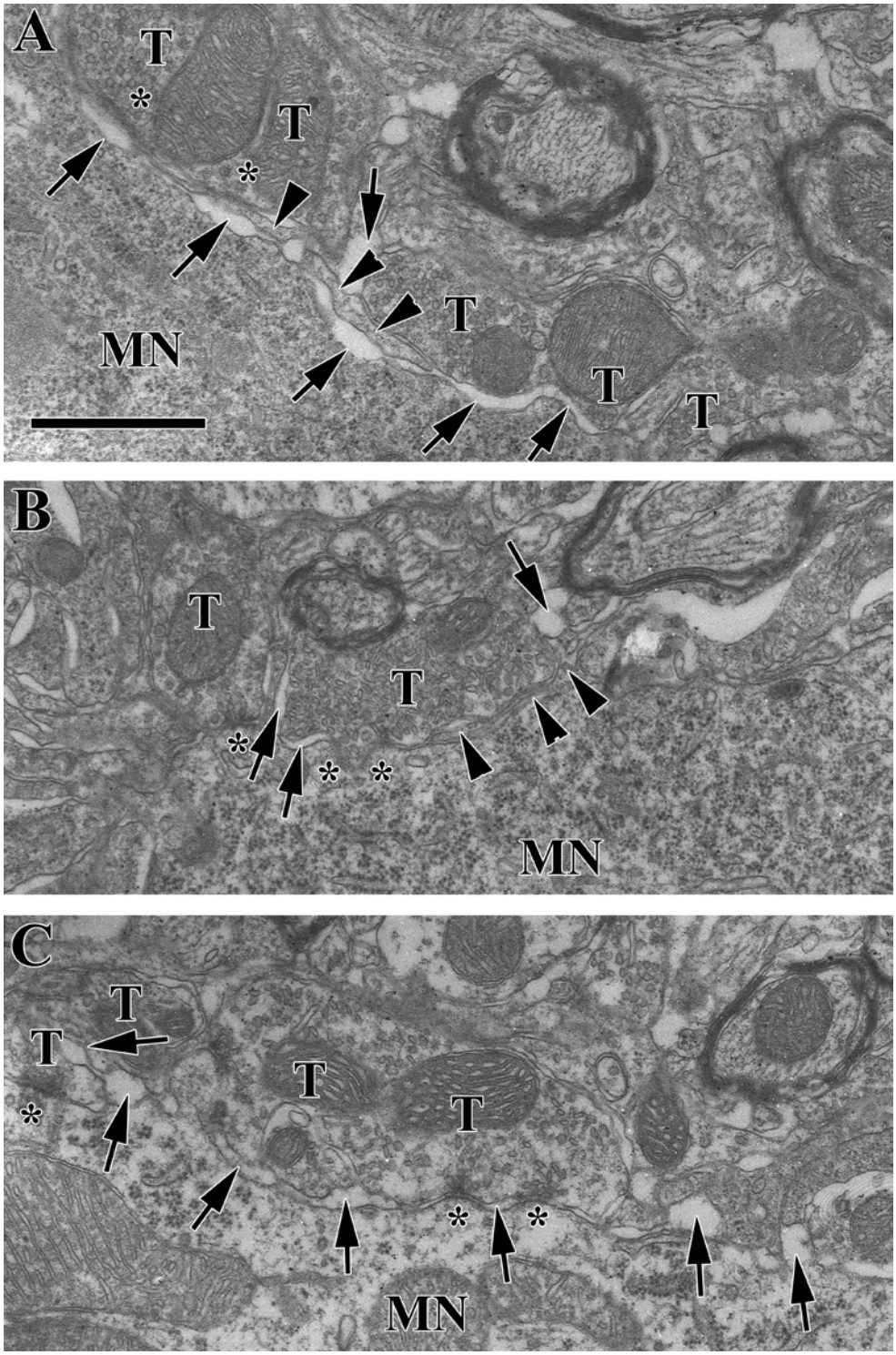
A
T
T
T
T
T
MN
B
T
T
MN
C
T
T
T
T
T
MN

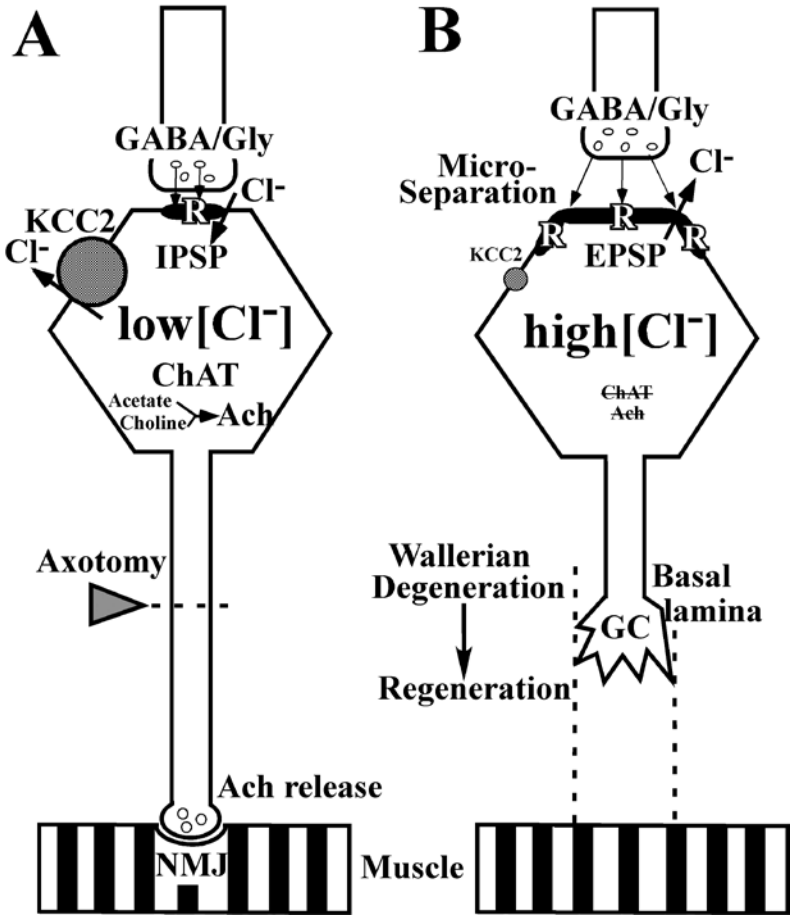
A
GABA/Gly
Cl-
R
KCC2
Cl-
IPSP
low[Cl-]
ChAT
Acetate
Choline
Ach
Axotomy
Ach release
NMJ
Muscle
B
GABA/Gly
Micro-
Separation
Cl-
R
R
R
KCC2
EPSP
high[Cl-]
ChAT
Ach
Wallerian
Degeneration
Basal
lamina
GC
Regeneration

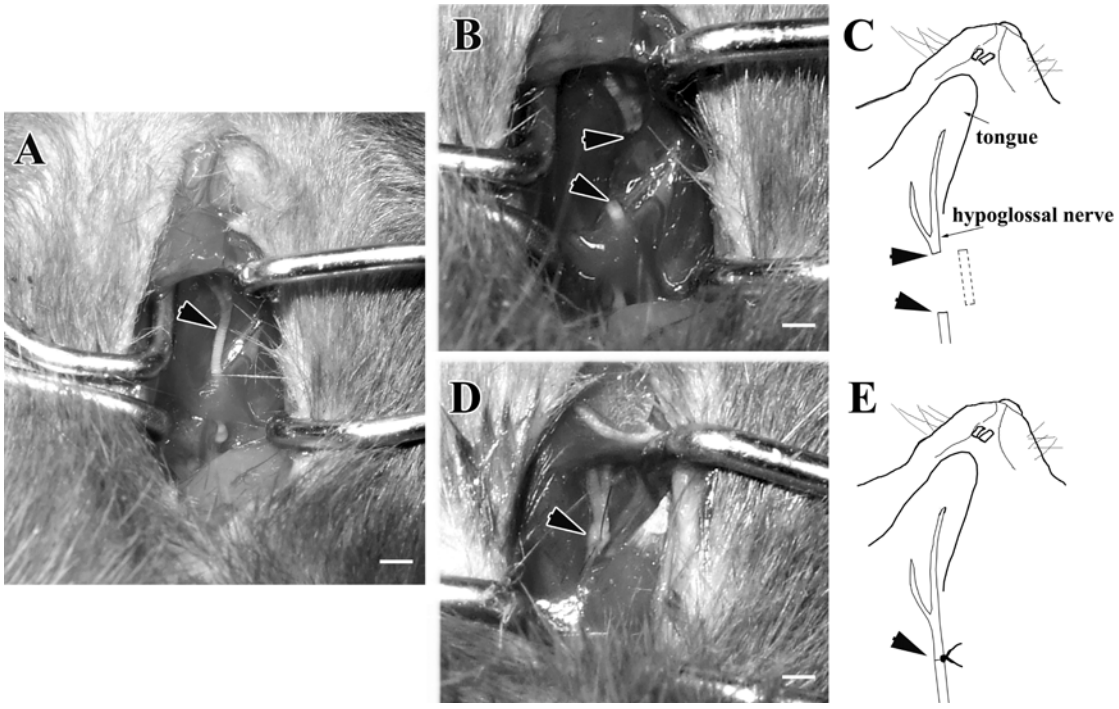
A
B
C
tongue
hypoglossal nerve
D
E